

Received June 29, 2016; reviewed; accepted September 7, 2017

## SUPPORT PARAMETERS OPTIMIZATION AND ENGINEERING APPLICATION OF ROADWAY WITH BROKEN-EXPAND SURROUNDING ROCK IN DEEP

W.J. YU<sup>1,2\*</sup>, G.S. WU<sup>2</sup>

<sup>1</sup> Key Laboratory of Safe and Effective Coal Mining (Anhui University of Science and Technology), Ministry of Education, Huainan, Anhui 232001, China

<sup>2</sup> School of resource, environment and safety engineering, Hunan University of Science and Technology, Xiangtan, Hunan 411201, China

**Abstract:** Aiming at the deformation characteristics and the support problem of deep high stress broken-expand surrounding rock, the secondary support of the deep roadway engineering of Fenglong coal mine in Jiangxi Province, China, is carried out to optimize the parameters. First of all, according to the characteristics of deep roadway deformation in Fenglong coal mine, the specific support scheme was put forward on the basis of the original support, then, the secondary support parameters and the support time are designed. The softening strength parameters of the surrounding rock in the roadway are obtained by using the piecewise linear strain softening model and the dilatancy angle of the rock mass. Considering the strength effect of cable anchor, the calculation equation and support strength index ID concept of anchor cable are put forward, and the corrected calculation parameters of anchorage effect are given. Then, the numerical calculation is carried out for 16 schemes, meanwhile, the optimal scheme of the comprehensive evaluation index  $E_s$  of roadway engineering stability is adopted. The influence of different anchoring effect on the stability of roadway and different secondary displacement value on the stability of roadway are analyzed respectively. Finally, the optimized support scheme is used to carry out the engineering practice, the results of monitoring the deformation of roadway by cross method show that the deformation value is within the controllable range, which can better control the roadway deformation.

**Keywords:** high stress, secondary support, optimization of support parameters, numerical calculation, surrounding rock

\* Corresponding author: [ywjlah@163.com](mailto:ywjlah@163.com) (W.J. Yu)

## 1. INTRODUCTION

After the deep high stress rock mass has been excavated, then, a large number of cracks in the surrounding rock were rapidly expanding. Moreover, this phenomenon has the characteristics of fast deformation speed, large deformation and long duration of deformation. At present, the stability and control technology of the surrounding rock of such engineering has become a hot and difficult problem (Yu et al. 2017; 2015; 2014a). Such as G.C. Zhang and He (2015) proposed a multi-level coupling support system with high strength anchor cable and net, retractable ring bracket and grouting reinforcement as core based on the stress dilatancy expansion (HJS) composite geologic soft rock, then, the concrete support form of coupling mechanism of the surrounding rock and the design of supporting parameters were analyzed. X.F. Li et al. (2014) designed a bolt-mesh-anchor coupling support for the roadway repair and reinforcement, which consists of a first coupling support with bolt-mesh and secondary reinforcement with anchor cables. R.S. Yang et al. (2017) proposed a support technology focusing on cutting off the water, strengthening the small structure of the rock and transferring the large structure of the rock. Z.Q. Zhao et al. (2016) analyzed the uneven evolution law of the mining stress field and its plastic zone characteristics of the roadway under the action based on the butterfly shape plastic zone theory of roadway surrounding rock. J.B. Bai and C.J. Hou (2006) studied the stability of surrounding rock in deep roadway, and believed that the basic method of surrounding rock control in deep roadway is to improve the strength of surrounding rock, transfer high stress of surrounding rock and adopt reasonable support technology. S.J. Niu et al. (2012) studied the strength attenuation law of broken surrounding rock in deep roadway. T.Q. Xiao et al. (2011) put forward the high pretension bolt and diagonal cable and beam combined support surrounding rock control technology based on the mechanism of shear failure in the form of “inverted trapezoidal” plastic zone. H.P. Kang et al. (2007) proposed high prestress and power support theory based on the conditions of deep coal mine and complicated roadway which greatly improve the supporting system of the initial supporting stiffness and strength, maintain the integrity of surrounding rock and reduce the reduction of the surrounding rock strength. W.J. Wang et al. (2006) analyzed the deformation characteristics of surrounding rock and the failure reasons of support in deep coal seam roadway, and then, put forward the internal and external structure coupling balanced support principle of this kind of roadway. W.J. Yu et al. (2014b) also studied the deformation mechanism and control technology of repair, and then, proposed anchorage length formula and the main parameters of repairing roadway aiming at the high stress of soft rock roadway with large deformation and failure problems. The above research provides a better theoretical basis and control measures for the problems such as rapid deformation, long deformation time and difficult support in deep high stress rock mass.

The design of the deep roadway surrounding rock support often need to consider secondary or more support, the permanent support parameters is particularly important to

the long-term stability of the roadway surrounding rock for a long service. In the design of supporting parameters, J.C. Chang et al. (2012) proposed the anchor-cable should be installed at good time with bolts supporting after roadway driving because it can improve the stress states of deep surrounding rock around the roadway and control the roadway deformation effectively. H.T. Liu and J.T. Li (2015) studied the deformation law and characteristics of the bolting and shotcreting-anchor cable-anchor grouting support system in different support periods, and the reasonable combined support of the unit was obtained. Q.L. Chang et al. (2007) put forward a mechanical model of the first bolting net and the seconded stone arch support from the perspective of macro and micro mechanical properties of rock composition. N. Zhang et al. (2010) used the intrinsically safe YTJ20-type drilling peers TV imaging and dyeing agent tracking slurry method for the problem of roadway hysteresis grouting effect is difficult to be guaranteed, the Zhuji coal mine anchor bolt support conditions under the effect of lagging grouting in deep well soft rock roadway is tested. Y.M. Li et al. (2015) analyzed the support process of stress and strength adjustment in soft surrounding rock roadway based on the principle of soft rock roadway support, and determined the theoretical formula of the optimal time of secondary support, and so on. The above study has emphasized the importance of the secondary support parameters and the support time, however, it is difficult to grasp the best supporting time, and there is no clear definition of the secondary support time. Especially, the optimization and research results of the secondary support parameters and the support time which taken into consideration are still rare.

Therefore, this paper based on the deep roadway engineering of Fenglong coal mine in Jiangxi Province, China. Then, on the basis of the original scheme, the mainly optimization design of the parameters for the secondary support is carried out, and the optimum support scheme is obtained and applied.

## 2. PROJECT OVERVIEW

The No. 209 mining area wind stone gate roadway section shape is the semi-circular arch in Jiangxi Fenglong coal mine north wing -800 m level, with net width × net height of 4.4 m × 3.5 m, and cross-section of 13.3 m<sup>2</sup>. The main faults in the area including DF<sub>4</sub>, DF<sub>5</sub> and DF<sub>9</sub>, respectively. Besides, the surrounding rock is a small block of Maokou limestone, a mixture of carbonaceous mudstone and mudstone (Fig. 1). The rock formation is disordered and the joints and fissures are developed with a depth of 840 m, which belongs to a typical high stress fractured rock mass.

The mineral composition analysis of the rock formation by X-ray diffraction shows that the content of montmorillonite can reach 36% (Fig. 2). Field investigation of similar project of coal mine (i.e., No. 207 mining area windstone roadway) has been carried out after the excavation, although the use of the “metal mesh, shotcrete, anchor bolt, anchor cable” joint support, and some parts even use high strength U-shaped

steel retractable support, however, due to the high stress level and coupled with broken rock, so that the roof spray and the surrounding rock have serious problems including separation, cracking, collapse and bulging and other phenomena. Figure 3 shows that the deformation of the surrounding rock in the roadway has the characteristics including large deformation, fast deformation speed and long duration of deformation, which has brought great negative influence to the mine production and seriously hindered the improvement of the productivity.

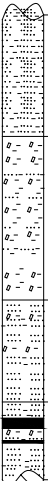
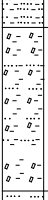
	Lithology	Thickness(m)	Description
	Siltstone	63.95	Gray siltstone and fine sandstone, thin layer, horizontal bedding development.
	Mudstone	78.94	Thin black mudstone, intercalated with siltstone. The structure is compact and homogeneous.
	Siltstone/ Mudstone	67.78	Light gray and deep gray siltstone, fine sand and mudstone.
	Siltstone	86.76	Dark gray siltstone, fine sandstone and mudstone.

Fig. 1. Generalized stratigraphic column

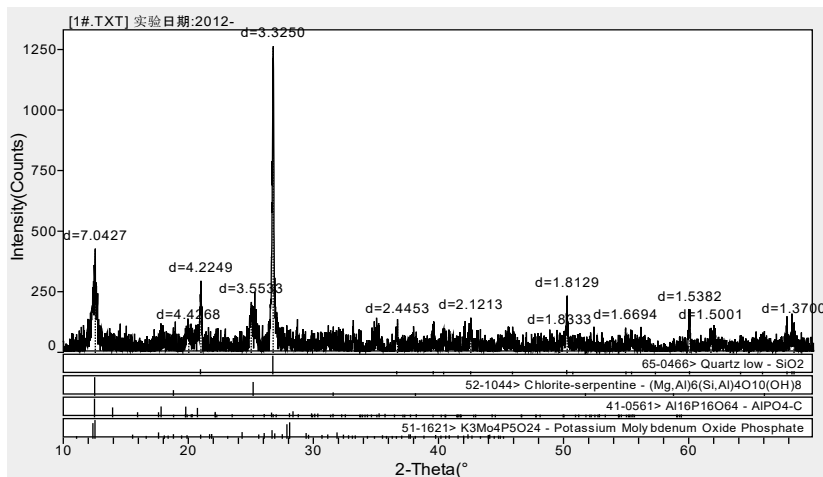


Fig. 2. Rock X-ray diffraction



Fig. 3. Actual deformation of surrounding rock and deep roadway section:  
a – the original roadway section, b – deformation of roadway surrounding rock

### 3. PARAMETERS AND SCHEME OF ROADWAY SUPPORT

#### 3.1. FIRST SUPPORT PARAMETER

The north wing -800 m level No. 209 mining area wind stone gate roadway is a permanent project, the support with “metal mesh, shotcrete, anchor bolt, anchor cable” jointed control technology. According to the characteristics of the project, the redesign is still in the original support on the basis using anchor cable, steel net, grouting, shotcrete and anchor cable to support the roadway. The specific support parameters are as follows: The roadway roof and sidewalls with full length grouting anchor bolt  $l_c$  is 2.5 m, and the row and line spacing is  $0.8 \text{ m} \times 0.8 \text{ m}$ ; Net spray layer thickness is 15cm, with concrete strength of C25; Anchor bolt made of the BHRB500 material left-hand longitudinal bar steel mesh. The whole section hanging wire mesh and steel ladder beam, metal mesh is 6.5 mm, grid is  $100 \times 100 \text{ mm}$ , specifications for  $1000 \times 800 \text{ mm}$ ; Metal mesh stubs must have the anchor bolt plus steel ladder beam which could be tightened and closed to the rock surface, the net between the length of not less than 100 mm, reinforced ladder beam made of 12 mm diameter round steel; Plate with the center of the prominent  $200 \text{ mm} \times 200 \text{ mm} \times 10 \text{ mm}$ . The roadway floor adopts selfdrilling grouting anchor bolt, the length of anchor is 2.0 m, the row and line spacing of bolt is  $0.8 \times 0.8 \text{ m}$ , respectively. The reinforcing steel net spraying layer is installed, the floor and the anchor bolt are connected into an integral whole.

#### 3.2. SECONDARY SUPPORT PARAMETER

The roof and the sidewalls are adopted anchor cable with the length of 6 m, 7 m, 8 m and 9 m respectively. Similarly, the row and line spacing are  $600 \text{ mm} \times 600 \text{ mm}$ ,

800 mm × 800 mm, 1000 mm × 1000 mm and 1200 mm × 1200 mm, respectively. Anchor cable length is 2500 mm with diameter of 17.8 mm, and the resin end anchorage is used. Each anchor cable using 5 volumes of model K2350 resin drugs, prestress force should be not less than 100 KN. The anchor plate is stacked with two mats; the specifications are 350 mm × 350 mm × 10 mm and 150 mm × 150 mm × 10 mm square plate.

### 3.3. SECONDARY SUPPORT TIME

The support time, i.e., the time interval between the two supports (or the time interval after excavation and support). In this paper, in order to indicate the macroscopic phenomenon of the timing of support more visually, the release displacement is used to illustrate this problem, which is called the support time shift displacement value  $d_a$ . Because of the large pressure and loose rock mass, the deformation speed of the roadway is faster and the deformation is larger after the excavation, therefore, the secondary support time is of great important. According to experience and facilitate the design, the displacement needs to be released from 0 to 100 mm before the completion of the second support. In the paper, the release displacement is set as 20 mm, 40 mm, 60 mm and 80 mm respectively.

### 3.4. SCHEME DESIGN

According to the above support parameters, the initial support parameters are original, and the secondary support parameters should consider the cable length  $l_a$ , the inter-row spacing  $e_a \times i_a$  and the secondary support time shift displacement value  $d_a$ ,

Table 1. Each influencing factor and its parameter level

Scheme factors		Parameter level	Number
Secondary support	Cable length $l_a$ , mm	1	6000
		2	7000
		3	8000
		4	9000
	Row and line space of cable $e_a \times i_a$ , mm × mm	1	600 × 600
		2	800 × 800
		3	1000 × 1000
		4	1200 × 1200
	Secondary support time shift displacement value $d_a$ , mm	1	20
		2	40
		3	60
		4	80

respectively. In order to minimize the calculation of the unnecessary schemes, the orthogonal test table is adopted for the design. In the paper, three factors (i.e., the cable length  $l_a$ , cable row and line spacing  $e_a \times i_a$  and secondary support time shift displacement value  $d_a$ ) should be considered its influence. According to the secondary support parameter design, each factor should consider four levels, and the four levels of each factor in the above design has been given, therefore, the secondary support program design can be used orthogonal test table L16 ( $4^3$ ), 16 calculation schemes were obtained (parameter level is shown in Table 1). Each calculation scheme is shown in Table 2.

Table 2. Support calculation scheme

Scheme	Cable length $l_a$ , mm	Row and line space of cable $e_a \times i_a$ , mm × mm	Secondary support time shift displacement value $d_a$ , mm
1	6000	600 × 600	20
2	6000	800 × 800	40
3	6000	1000 × 1000	60
4	6000	1200 × 1200	80
5	7000	600 × 600	20
6	7000	800 × 800	40
7	7000	1000 × 1000	60
8	7000	1200 × 1200	80
9	8000	600 × 600	20
10	8000	800 × 800	40
11	8000	1000 × 1000	60
12	8000	1200 × 1200	80
13	9000	600 × 600	20
14	9000	800 × 800	40
15	9000	1000 × 1000	60
16	9000	1200 × 1200	80

#### 4. OPTIMIZATION OF SUPPORT PARAMETERS FOR HIGH STRESS LARGE DEFORMATION ROADWAY

##### 4.1. NUMERICAL MODEL OF ROADWAY

The size length and width is 90 m × 90 m, the width and height is 4.4 m × 3.5 m of the roadway model. The left and right boundaries of the model are fixed  $X$ -axis displacement constrained boundary, the lower boundary is fixed  $X$  and  $Y$  axis displacement constraint boundary and the upper boundary is the stress boundary (Fig. 4), the uniform load is applied according to the thickness of the overlying strata (840 m). Based on the original stress results of Fenglong coal mine, the vertical stress is taken from the geostatic stress and the lateral pressure coefficient  $\lambda$  is 1.2.

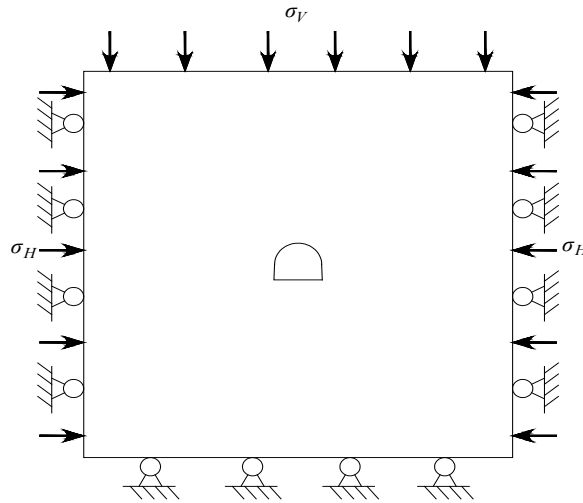


Fig. 4. Numerical calculation model of roadway

Table 3 gives the boundary values for calculating the stress boundary conditions of the model. In order to simulate the horizontal tectonic stress field, the initial stress field of the original rock is obtained by the iterative cycle that reaches the equilibrium state according to the given stress boundary condition and gives the gravity acceleration. Besides, in the case of calculation, the disturbance stress is 1.0–1.3 times of the stress of the original rock during mining in general. Therefore, the disturbance stress coefficient  $\beta$  (disturbance stress and the ratio of the original rock stress) are 1.0, 1.2, 1.4, respectively.

Table 3. Numerical calculation of boundary stress

Buried depth $H$ (m)	Buried depth of upper and lower boundary (m)		Coefficient of disturbance stress $\beta$	Vertical stress on the upper and lower borders $\sigma_v$ (MPa)		Vertical stress on left and right borders $\sigma_H$ (MPa)	
	Buried depth of upper boundary, $H_1$	Buried depth of lower boundary, $H_2$		Vertical stress on the upper boundary $\sigma_{v1}$	Vertical stress on the lower boundary $\sigma_{v2}$	Left and right border upper horizontal stress $\sigma_{H1}$	Left and right border lower horizontal stress $\sigma_{H2}$
840	795	885	1.0	19.875	22.125	23.850	26.550
			1.2	23.850	26.550	28.620	31.860
			1.4	27.825	30.975	33.390	37.170

Note: the average density of overlying rock mass in roadway is  $2500 \text{ kg/m}^3$ .

#### 4.2. CALCULATION PARAMETER

- (1) Raw rock calculation parameters. Based on the roadway geological survey, it was found that the rock mass in the roadway is basically in the class IV, the RMR value is between 30 and 40, thus the rock parameters are listed in Table 4.

Table 4. Calculation parameters for rock mass of wind stone gate roadway  
at No. 209 level of north wing -800 m level

Lithology	Bulk density $\gamma$ (kg/m <sup>3</sup> )	Compressive strength $R_c$ (MPa)	Tensile strength $R_t$ (MPa)	Cohesion $C$ (MPa)	Internal friction angle $\varphi$ (°)	Deformation modulus $E$ (GPa)	Poisson ratio $\mu$
Maokou limestone (Carbonaceous mudstone and mudstone)	2500	16.75	1.0	0.80	29.0	7.00	0.22

- (2) Calculation parameters of roadway surrounding rock. After the surrounding rock of the roadway has reached the yield strength, the shear strength and relaxation of the joint cracks not only reduce the surrounding rock strength rapidly, but also the volume expansion of the surrounding rock increased with the increase of the displacement. This volume expansion and intensity weakening effect are more pronounced for deep fractured rock mass. In order to simulate this rock mass effect, a piecewise linear strain softening model is used in the calculation, and the swelling effect of the rock mass is taken into account by the dilatancy angle of the rock mass. According to the experimental study, the rock expansion angle is 5°–20°. The plastic strain and rock mass strength parameters of the strain softening model of the No. 209 mining area wind stone gate roadway in the north wing -800 m level are shown in Table 5.

Table 5. Calculation parameters of post peak of roadway surrounding rock

Lithology	Bulk density $\gamma$ (kg/m <sup>3</sup> )	Compressive strength $R_{c1}$ (MPa)	Tensile strength $R_{t1}$ (MPa)	Cohesion $C_1$ (MPa)	Internal friction angle $\varphi_1$ (°)	Deformation modulus $E$ (GPa)	Poisson ratio $\mu$
Maokou limestone (Carbonaceous mudstone and mudstone)	2500	8.375	0.50	0.40	22.27	7.00	0.22

- (3) Bolt and cable calculation parameters. The corresponding mechanical parameters are calculated according to the diameter of the bolt, the anchorage method

(full length anchor or end anchor) and the row and line space. The mechanical parameters of anchor bolt, prestressed anchor cable and shotcrete layer are given in tables 6 and 7, respectively.

Table 6. Calculated parameters of the anchor bolt and anchor cable structure

Support structure	Diameter (mm)	Section area ( $10^{-4} \text{ m}^2$ )	Mortar compressive strength (MPa)	Elastic modulus (GPa)	Yield strength (kN)	$K_{\text{bond}}$ (GPa)	$S_{\text{bond}}$ ( $10^5 \text{ N}$ )
Bolt	22	3.80	20	98.6	130.0	31.3	5.65
Cable	17.8	2.13	20	49.3	115.0	3.25	2.4

Table 7. Calculated parameters of the concrete sprayed layer

Spray layer material	Spray layer thickness (m)	Section area ( $\text{m}^2$ )	Spray layer elastic modulus $E$ (GPa)	Section inertia moment $I$ ( $\text{m}^4$ )
Plain shotcrete	0.10	0.1	17.5	$83.3 \times 10^{-6}$
Metal mesh spraying layer	0.20	0.2	21.0	$666.7 \times 10^{-6}$

#### 4.3. STRENGTH EFFECT OF CABLE ANCHORAGE BODY

The anchoring effect of the anchor cable is mainly play a role to improve the carrying capacity of the surrounding rock by the applied lateral stress, meanwhile, because the anchorage body of the anchor cable has a high strength effect, a composite strengthening body is formed between the rock mass and the supporting member, which can greatly limit the severe deformation of surrounding rock. Therefore, the anchor body strength effect is to reduce the degree of weakening of the surrounding rock, i.e., increased the residual strength of the surrounding rock. In order to quantitatively consider the effect of the strength of the anchorage body, it is assumed that the effect is proportional to the length and pre-stress of the anchor and is inversely proportional to the product of the row and line space, whereby the support strength index  $ID$  of the anchor cable can be defined as follows:

$$ID = K_T \frac{l_c}{e_c \cdot i_c}. \quad (1)$$

Where,  $l_c$  is the anchor cable length (m);  $e_c$  and  $i_c$  are the row and line space of anchor cable respectively (m);  $K_T$  is the prestressed anchor cable correction coefficient, according to experience, the following correction coefficient expression is given:

$$K_T = 1 + \frac{1}{20} \cdot \frac{Q_c}{e_c \cdot i_c} \quad (2)$$

where,  $Q_c$  is the prestress force applied by a single anchor ( $t$ ), here, 14  $t$  is taken.

The application of anchor bolt, especially pre-stressed anchor cable, which increases the contact stress between the surrounding rocks, avoids or reduces the loose range and increases the residual strength of the plastic zone as well. In this paper, the anchoring effect correction parameters of the support surrounding rock are given as follows:

$$R_c^P = R_{c_1} \left( 1 + \frac{ID}{10} \right), \quad (3)$$

$$R_t^P = R_{t_1} \left( 1 + \frac{ID}{10} \right), \quad (4)$$

$$C_1 = C_1 \left( 1 + \frac{ID}{10} \right), \quad (5)$$

$$\operatorname{tg} \varphi^P = \left( 1 + \frac{ID}{10} \right) \operatorname{tg} \varphi_1, \quad (6)$$

where,  $R_c^P$ ,  $R_t^P$ ,  $C^P$  and  $\varphi^P$  are the correction parameter of compressive strength, tensile strength, cohesive force and internal friction angle after the post-peak of surrounding rock respectively;  $R_{c_1}$ ,  $R_{t_1}$ ,  $C_1$  and  $\varphi_1$  are mechanical calculation parameters for softening the surrounding rock after peak respectively as shown in Table 6.

According to Eqs. (3)–(6), the value of the supporting strength index  $ID$  with different support schemes and parameters of rock strength after corresponding plastic strain peaks are obtained, as shown in Table 8.

Table 8. Calculation parameters of rock mass modified by anchoring effect of surrounding rock after secondary support

Scheme	Supporting strength index $ID$	Compressive strength (MPa)	Tensile strength (MPa)	Cohesion (MPa)	Internal friction angle ( $^\circ$ )	Deformation modulus (GPa)	Poisson ratio
1	2	3	4	5	5	6	7
1	16.70	22.36	1.33	1.07	47.55	7.00	0.22
2	9.39	16.24	0.97	0.78	38.44	7.00	0.22
3	6.00	13.40	0.80	0.64	33.24	7.00	0.22
4	4.17	11.87	0.71	0.57	30.12	7.00	0.22

<b>1</b>	<b>2</b>	<b>3</b>	<b>4</b>	<b>5</b>	<b>6</b>	<b>7</b>	<b>8</b>
5	19.48	24.69	1.47	1.18	50.37	7.00	0.22
6	10.95	17.55	1.05	0.84	40.63	7.00	0.22
7	7.00	14.24	0.85	0.68	34.85	7.00	0.22
8	4.86	12.45	0.74	0.59	31.33	7.00	0.22
9	22.27	27.02	1.61	1.29	52.88	7.00	0.22
10	12.51	18.86	1.13	0.90	42.68	7.00	0.22
11	8.01	15.08	0.90	0.72	36.40	7.00	0.22
12	5.56	13.03	0.78	0.62	32.50	7.00	0.22
13	25.05	29.35	1.75	1.40	55.13	7.00	0.22
14	14.08	20.17	1.20	0.96	44.60	7.00	0.22
15	9.01	15.92	0.95	0.76	37.90	7.00	0.22
16	6.25	13.61	0.81	0.65	33.65	7.00	0.22

#### 4.4. EVALUATION INDEX OF ROADWAY STABILITY

In general, the stability of the surrounding rock is related to the stress release, it is mainly shown in the following two points: Firstly, a certain range loose zone is from outside to inside in the roadway. The second is the release of surrounding rock stress and the internal stress of rock mass decrease with the development of the loose zone of surrounding rock, however, the resistance of supporting structure is increasing. Therefore, it can be considered that when the final bearing resistance  $R_{\text{last}}$  of the support structure is less than the ultimate resistance  $R_{\text{max}}$  of the support structure can sustain, the stability of the roadway surrounding rock is inversely proportional to the maximum monitoring displacement  $U_{\text{max}}$ , the final convergence rate  $V_c$  and the plastic zone range  $P$ , conversely, which directly proportional to the final bearing resistance of the support structure  $R_{\text{last}}$  and safety factor  $F_s$ . That is, the comprehensive evaluation index of the stability of roadway engineering can be expressed as:

$$E_s = k \frac{R_{\text{last}} \cdot F_s}{V_c \cdot P \cdot U_{\text{max}}}, \quad (7)$$

where,  $E_s$  is the comprehensive score of the stability of the roadway engineering,  $k$  is the normalization coefficient, the maximum value of the  $E_s$  is 1,  $R_{\text{last}}$  is the final bearing resistance of the support structure, MPa,  $U_{\text{max}}$  is the maximum monitoring displacement of the roadway surrounding rock, m,  $V_c$  is the final convergence rate of the surrounding rock, m/step,  $P$  is the plastic zone, m,  $F_s$  is the safety factor.

## 5. CALCULATION RESULT

The results obtained from the 16 schemes in Table 2 are shown in Table 9. Figure 5 illustrates the Eq. (7) available in the program's comprehensive score value. Schemes 9, 10 and 13 have a higher combined score of 0.89, 0.77 and 1.00, respectively. Therefore, these three schemes can be used as the best alternatives. According to the needs of the field, schemes 9 and 10 have a relatively close score. Similarly, all the factors including the displacement, convergence rate, plastic zone and the resistance of support structure and safety factor (i.e., all more than 1.5), all the calculation results are relatively close, that these two programs can guarantee the stability of the roadway. However, from an economic point of view, the No. 10 scheme can save a part of the cost compared with the No. 9 scheme, therefore, taking into account a variety of factors, the No. 10 scheme is optimal, i.e., the cable length  $l_c$  is 8000 mm, row and line space  $e_c \times i_c$  is 800 mm × 800 mm, initial support time displacement value of  $d_c$  is 40 mm, respectively.

Table 9. Evaluation index value of each scheme

Scheme	Maximum monitoring displacement $U_{\max}$ (mm)			Final convergence rate $V_c$ (mm/step)			Final bearing resistance of the support structure $R_{last}$ (MPa)	Plastic zone of surrounding rock $P$ (m)	Safety factor $F_s$
	Vault	Sidewalls	Floor	Vault	Sidewalls	Floor			
1	216.8	221.1	227.3	$2.98 \times 10^{-4}$	$3.25 \times 10^{-4}$	$3.23 \times 10^{-4}$	13.24	6.32	1.24
2	257.1	269.1	298.4	$1.78 \times 10^{-4}$	$1.17 \times 10^{-4}$	$2.23 \times 10^{-4}$	13.12	6.58	1.21
3	317.2	338.1	341.9	$1.44 \times 10^{-4}$	$1.45 \times 10^{-4}$	$1.98 \times 10^{-4}$	12.36	6.97	1.19
4	358.1	389.4	354.1	$2.97 \times 10^{-4}$	$2.80 \times 10^{-4}$	$1.88 \times 10^{-4}$	13.18	7.21	1.17
5	208.1	211.8	217.2	$2.59 \times 10^{-4}$	$2.84 \times 10^{-4}$	$2.87 \times 10^{-4}$	11.47	5.59	1.34
6	241.9	254.3	284.6	$2.64 \times 10^{-4}$	$2.89 \times 10^{-4}$	$2.01 \times 10^{-4}$	11.97	6.12	1.31
7	298.4	321.4	321.9	$1.27 \times 10^{-4}$	$2.01 \times 10^{-4}$	$1.58 \times 10^{-4}$	10.25	7.47	1.24
8	331.6	358.3	334.7	$2.04 \times 10^{-4}$	$2.41 \times 10^{-4}$	$2.18 \times 10^{-4}$	11.11	7.01	1.19
9	195.8	204.4	207.9	$2.01 \times 10^{-4}$	$2.61 \times 10^{-4}$	$2.42 \times 10^{-4}$	11.87	4.36	1.51
10	232.0	247.2	254.4	$1.92 \times 10^{-4}$	$1.97 \times 10^{-4}$	$1.84 \times 10^{-4}$	11.05	4.87	1.53
11	274.1	303.5	297.0	$2.37 \times 10^{-4}$	$2.79 \times 10^{-4}$	$1.99 \times 10^{-4}$	9.66	5.74	1.38
12	318.9	337.5	326.4	$1.25 \times 10^{-4}$	$1.94 \times 10^{-4}$	$1.35 \times 10^{-4}$	10.93	6.23	1.34
13	167.4	189.6	184.0	$2.24 \times 10^{-4}$	$2.19 \times 10^{-4}$	$2.20 \times 10^{-4}$	10.67	4.21	1.52
14	217.8	219.6	227.7	$2.92 \times 10^{-4}$	$2.87 \times 10^{-4}$	$2.64 \times 10^{-4}$	10.49	4.41	1.57
15	249.5	273.5	254.6	$2.08 \times 10^{-4}$	$2.67 \times 10^{-4}$	$2.67 \times 10^{-4}$	9.34	4.94	1.43
16	297.3	309.2	296.9	$2.44 \times 10^{-4}$	$2.83 \times 10^{-4}$	$2.68 \times 10^{-4}$	11.38	5.58	1.36

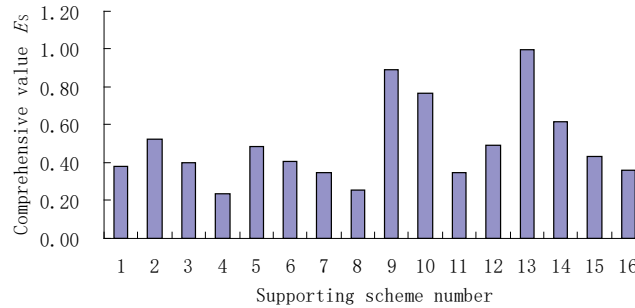
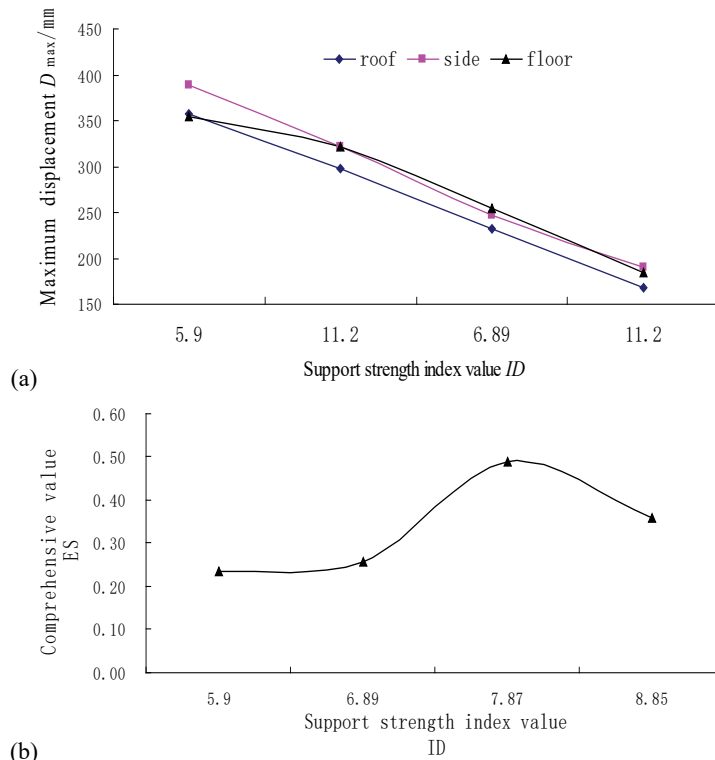


Fig. 5. The composite score of each calculation scheme

### 5.1. INFLUENCE OF DIFFERENT ANCHORING EFFECTS ON ROADWAY STABILITY

In general, the greater the support strength index  $ID$  value, the better the anchoring effect and the smaller the deformation of the surrounding rock, in other words, the more stable the roadway. In fact, according to the relationship between the support

Fig. 6. The relationship between different support strength index value  $ID$  and roadway stability

strength index  $ID$  and the roadway rock displacement value  $D_{\max}$  and the comprehensive score  $E_s$  (Fig. 6). It is found that although the deformation of the surrounding rock was gradually smaller with the increase of the support strength, the  $E_s$  value of the comprehensive score of the roadway engineering was no longer increased or even reduced which in a certain extent. Moreover, the stability of roadway with different surrounding rock quality increases with the length of anchor cable, and its stability safety coefficient is linear with the length of anchor cable. The stability of the roadway decreases with the mining stress, and the decreasing trend is also linear.

## 6. ENGINEERING PRACTICE

### 6.1. SUPPORT SCHEME

The first support based on the original support, by contrast, the cable parameters of the secondary support are determined by the above optimization results, i.e., the anchors cables diameter is 17.8 mm in the sidewalls and roof, the length of the cable is 8000 mm, the row and line space is 800 mm  $\times$  800 mm, respectively.

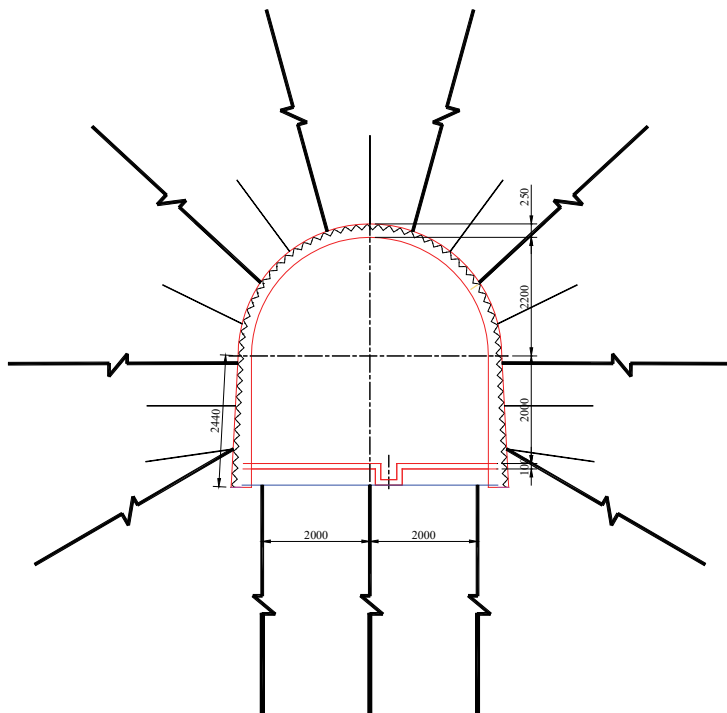


Fig. 7. Anchor cable support parameter

In addition, in order to control the deformation of the floor, the row and line space of the cable in the floor is set as 2000 mm × 1600 mm. The floor anchor cable is connected by long beam channel (4.4 m) and the two cables are formed as a whole. Besides, the floor anchor cable is arranged with an angle of 45° to the horizontal. Using resin end anchor, and the anchor length is 2500 mm. Each anchor cable using 5 volumes of model K2350 resin drugs, prestressing force shall be no less than 100 KN. The cable plate is stacked with two plate, the specifications are 350 mm × 350 mm × 10 mm and 150 mm × 150 mm × 10 mm square plate respectively, the larger plate is on the small plate, which as shown in Fig. 7.

## 6.2. FIELD MONITORING AND SUPPORT EFFECT

Cross section method is used to observe the deformation of the roadway and 4 monitoring points are arranged. The average values of the measured points as shown in Fig. 8. After 120 days of monitoring, the average convergence value of the sidewalls is 230 mm and the relative value of the roof to floor is 381 mm. The deformation value is within the controllable range, and the deformation tends to be stable, at the same time, the convergence rate is less than 1 mm/d at the later stage of monitoring. Therefore, through this optimization of the support scheme can better control the roadway deformation.

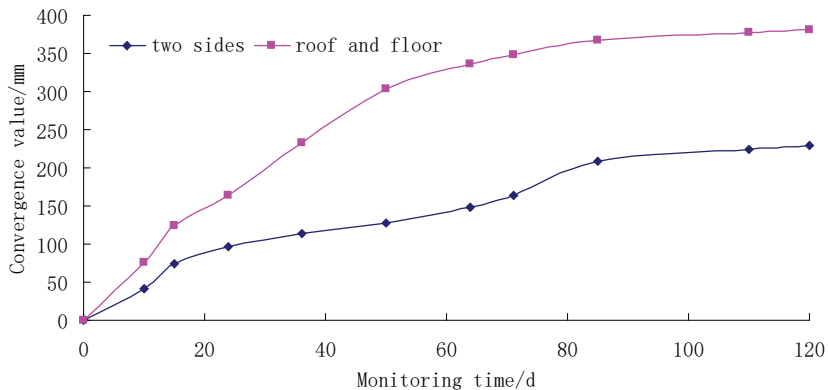


Fig. 8. Monitoring curve of roadway surrounding rock in test section

## 7. CONCLUSIONS

Based on the deep roadway engineering of Fenglong coal mine in Jiangxi Province, China. Then, the mainly optimization design of the parameters for the secondary support is carried out, we can obtain the optimum support scheme. The main conclusions are as follows:

- (1) On the basis of the original support scheme, the specific support parameters are put forward. Meanwhile, the secondary support parameters and the secondary support time are mainly considered. The length of the anchor cable  $l_a$ , the row and line space of the anchor cable  $e_a \times i_a$  and the displacement value of secondary support time  $d_a$  are considered respectively.
- (2) Based on the deep high stress deformation characteristics of broken expand rock, considering the effect of crushing deformation. The piecewise linear strain-softening model was used to obtain post-peak soften strength parameters of surrounding rock. The support strength index  $ID$  concept of cable, calculation equation and corrected calculation parameters of anchorage effect are given.
- (3) According to the relationship between the support strength index  $ID$  and the roadway rock displacement value  $D_{\max}$  and the comprehensive score  $E_s$ . Although the deformation of the surrounding rock was gradually smaller with the increase of the support strength, the  $E_s$  value of the comprehensive score of the roadway engineering was no longer increased or even reduced which in a certain extent.
- (4) The engineering practice shows that under the optimized secondary support parameters, the average convergence value of the sidewalls is 230 mm and the relative value of the roof to floor is 381mm. The deformation value is within the controllable range, and the deformation tends to be stable. Therefore, through this optimization of the support program can better control the roadway deformation.

#### ACKNOWLEDGMENTS

This study was supported by the Open Research Foundation of Key Laboratory of Safety and High-efficiency Coal Mining, Ministry of Education(Anhui University of Science and Technology) (JYBSYS2015201) and National Natural Science Foundation of China (51574122, 51434006). The financial supports are greatly appreciated.

#### REFERENCES

- BAI J.B., HOU C.J., 2006, *Control principle of surrounding rocks in deep roadway and its application*, Journal of China University of Mining and Technology, 35 (2), 145–148.
- CHANG J.C., XIE G.X., 2012, *Research on space-time coupling action laws of anchor-cable strengthening supporting for rock roadway in deep coal mine*, Journal of Coal Science & Engineering, 18 (2), 113–117.
- CHANG Q.L., ZHOU H.Q., LI D.W. et al., 2007, *Stability Principle of Extremely Rigid Secondary Support for Soft and Broken Rock Roadway*, Journal of Mining and Safety Engineering, 24 (2), 169–172.
- KANG H.P., WANG J.H., LIN J., 2007, *High pretension stress and intensive bolting system and its application in deep roadways*, Journal of China Coal Society, 32 (12), 1233–1238.
- LI X.F., CHENG G.H., LI X.Q. et al., 2014, *A Study of Soft Rock Roadway Coupling Support in Xiaojing Coal Mine*, Procedia Engineering, 84, 812–817.
- LI Y.M., ZHANG H., MENG X.R., 2015, *Research on secondary support time of soft rock roadway*, Journal of China Coal Society, 40 (s1), 47–52.

- LIU H.T., LI J.Q., 2015, *Research on timeliness of coordination support of bolting-mesh-shotcreting-grouting in deep roadway*, Journal of China Coal Society, 40 (10), 2347–2354.
- NIU S.J., JING H.W., YANG X.X. et al., 2012, *Experimental study of strength degradation law of surrounding rock in fractured zone of deep roadway*, Chinese Journal of Rock Mechanics and Engineering, (08), 1587–1596.
- WANG W.J., LI S.Q., OUYANG G.B., 2006, *Study on technique and test of surrounding rock control of deep shaft coal roadway*, Chinese Journal of Rock Mechanics and Engineering, 25 (10), 2102–2107.
- XIAO T.Q., BAI J.B., WANG X.Y. et al., 2011, *Stability principle and control of surrounding rock in deep coal roadway with large section and thick top-coal*, Rock and Soil Mechanics, 32 (6), 1874–1880.
- YANG R.S., LI Y.L., GUO D.M. et al., 2017, *Failure mechanism and control technology of water-immersed roadway in high-stress and soft rock in a deep mine*, International Journal of Mining Science and Technology, 27 (2), 245–252.
- YU W.J., WANG P., DU S.H., 2014a, *Deformation mechanism of high-stress and broken-expansion surrounding rock and supporting optimization based on the gray correlation theory*, Journal of Chongqing University (English Edition), 13 (3), 99–114.
- YU W.J., WANG W.J., HUANG W.Z. et al., 2014b, *Deformation mechanism and rework control technology of high stress and soft rock roadway*, Journal of China Coal Society, 39 (4), 614–623.
- YU W.J., WANG W.J., WU G.S. et al., 2017, *Three Zones and Support Technique for Large Section Incline Shaft Crossing Goaf*, Geotechnical & Geological Engineering, 1, 1–11.
- YU W.J., WANG W.J., CHEN X.Y. et al., 2015, *Field investigations of high-stress soft surrounding rocks and deformation control*, Journal of Rock Mechanics and Geotechnical Engineering, 7 (4), 421–433.
- ZHANG G.C., HE F.L., 2015, *Deformation failure mechanism of high stress deep soft roadway and its control*, Journal of Mining and Safety Engineering, 32 (4), 571–577.
- ZHANG N., WANG B.G., ZHENG X.G. et al., 2010, *Analysis on Grouting Reinforcement Results in Secondary Support of Soft Rock Roadway in Kilometre Deep Mine*, Coal Science and Technology, 38 (5), 34–38.
- ZHAO Z.Q., MA N.J., GUO X.F. et al., 2016, *Falling principle and support design of butterfly-failure roof in large deformation mining roadways*, Journal of China Coal Society, 41 (12), 2932–2939.